

A Framework for Reliability and Performance Assessment of Wind Energy Conversion Systems

Sebastian S. Smater, *Member, IEEE*, Alejandro D. Domínguez-García, *Member, IEEE*

Abstract—This paper proposes a framework for reliability and dynamic performance assessment of wind energy conversion systems (WECS) in the face of internal component faults and external grid disturbances. The proposed framework facilitates a quantitative analysis of different WECS designs, control strategies, and fault ride-through mechanisms. The framework can also be used to identify key design parameters that influence overall WECS reliability and to compute WECS reliability for different grid codes and performance requirements. To illustrate the framework, a case study for a doubly-fed induction generator is presented.

Index Terms—Reliability, Dynamic Performance, Wind Power, Wind Energy Conversion System (WECS), Doubly-Fed Induction Generator (DFIG), Low Voltage Ride-Through (LVRT).

I. INTRODUCTION

HIGH fossil fuel prices coupled with favorable political and socio-economic conditions have increased the adoption of renewable energy systems in recent years. The construction of wind farms with dozens of wind energy conversion systems (WECS) is economically feasible and leads to relatively large amounts of generated power. Hence, many utilities have increased their investment in wind power. There are several issues that must be addressed to enable deeper penetration of wind-based generation. According to the U.S. Department of Energy, achieving 20% of wind power penetration in the U.S. by 2030 will require: i) enhancement of the transmission infrastructure, ii) increased U.S. manufacturing capacity of wind generation equipment, and iii) improvement of reliability and operability of WECS [1].

Focusing on the last problem, there are three reliability-related issues that still hinder the widespread penetration of wind-based power generation [2]. These are i) the impact of wind speed variability on WECS reliability; ii) WECS reaction to grid disturbances; and iii) reliability of internal WECS components. In this paper, we argue that these three issues should not be treated separately when analyzing WECS reliability, and present a framework that attempts their integration. The conceptual framework over which this paper builds on was introduced in [3]. This paper substantially expands [3] by providing i) a more detailed description and a precise mathematical formulation of the proposed framework building blocks, and ii) a detailed case-study illustrating the application of the proposed framework.

To capture overall WECS reliability, it is necessary to compute a unifying reliability measure. This reliability measure characterizes a particular WECS working under specified conditions (grid characteristics) and specified fault types. In order to compute this reliability measure, detailed models of WECS, grid, and operating conditions are needed. These models can be both deterministic and probabilistic.

We review existing literature in reliability analysis methods for each of the three reliability-related issues mentioned above. The impact of wind variability on system reliability has been widely investigated using both, simulation-based and analytical methods. For example, in [4], probability distributions for the demand and the wind generation are used to formulate a reliability model, and a probabilistic binary model is used to describe WECS availability, i.e., the unit is either fully operational or completely failed. The objective was to find an optimal operational point that maximizes reliability and minimizes cost. In [5], conventional power system reliability analysis tools are used together with a model of the wind power plant. Even though this approach has little in common with our framework (it does not explicitly consider machine dynamics), it is worth emphasizing that it attempts to unify the reliability analysis of the power system together with the reliability analysis of wind power plants. The studies presented in [6], [7], [8] utilize Markov chains to describe power generation changes and generator failures. Using slightly different approaches to the ones discussed in [4], [5], they present a method to compute reliability measures, such as loss of load probability or loss of load expectation curves. There is also extensive work in reliability assessment of hybrid power generation systems. For example, in [9], reliability of a system consisting of WECS, diesel engines and batteries is analyzed, while [10] assesses the reliability of a microgrid with photovoltaic panels and WECS.

Work on WECS reaction to grid disturbances is mainly focused on development of mechanisms to withstand these disturbances, e.g., low voltage ride through (LVRT) [11], [12]. The work in [11] proposes the utilization of a series of braking resistors that could help dissipate the additional energy stored in rotor circuits during the fault. In [12], a rotor protection device is presented that is activated during a fault to connect the rotor converter in parallel with the grid-side converter. Additionally, many researchers have acknowledged that future WECS must adjust to grid standards—not the other way around—as seen in the large number of publications involving WECS control. Hence, different control strategies and designs of WECS include: real power control for smoothing shaft fluctuations [13], control strategies incorporating

S. Smater is with the Planning Department of the Electric Reliability Council of Texas, Taylor, TX 76574. Email: ssmater@ERCOT.COM

A. D. Domínguez-García is with the Department of Electrical and Computer Engineering of the University of Illinois at Urbana-Champaign, Urbana, IL 61801. Email: aledan@ILLINOIS.EDU

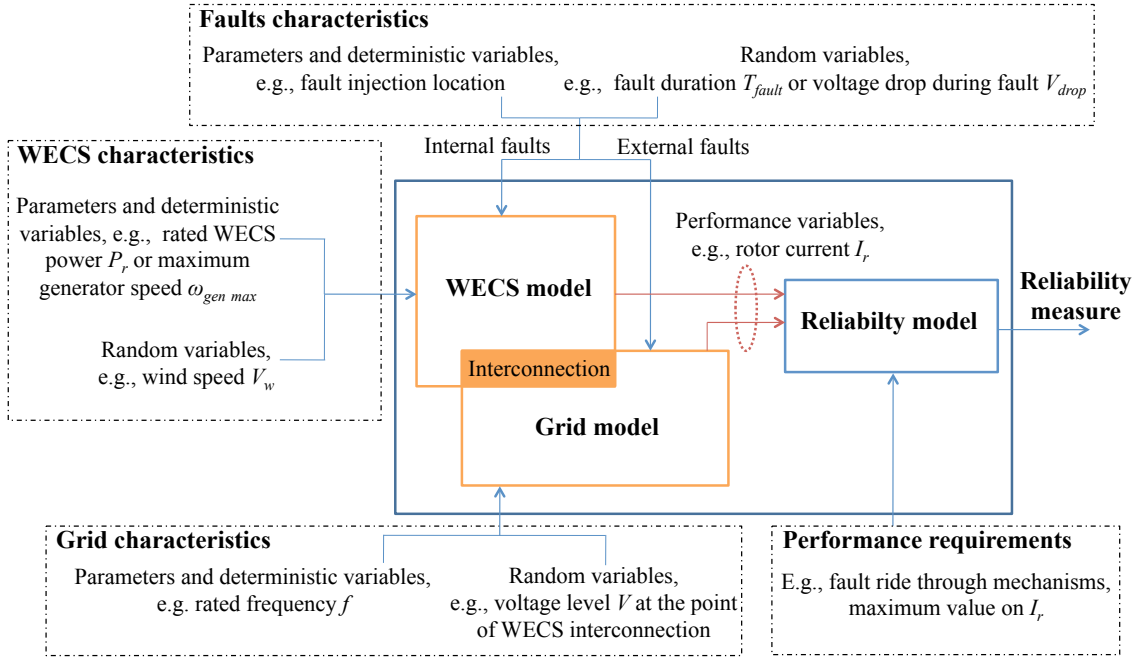


Fig. 1. Framework for reliability and dynamic performance assessment of wind energy conversion systems.

core saturation [14], and control to minimize the impact of inter-area oscillations [15]. While these works analyze the effectiveness of the proposed mechanisms, the analysis is conducted for a few specific scenarios without considering all possible operating conditions that a WECS might encounter. Furthermore, since WECS designs have to adjust to grid standards, reliability analysis cannot be performed only on the WECS model, but also on the grid model. Additionally, WECS and the grid must be modeled precisely, as their coupling may influence overall reliability.

At the WECS level, statistical data of individual components have been used for assessing reliability of individual WECS, disregarding the correlation between failures in each of those components and faults in the grid [16]. A similar approach can be found in [17], where the failure rate of WECS components is calculated based on their nominal failure rate and environmental stress factors, such as temperature. Reliability of WECS computed in this manner disregards any correlation between component failures. Finally, this method does not include grid fault events, which can cause a much faster component degradation than failure rates would suggest.

In this paper, we introduce a framework for reliability and dynamic performance analysis of WECS, which will provide an overall measure of reliability for a particular WECS operating under all possible conditions, and subject to all possible faults (in the WECS and the grid). In the proposed framework, the WECS/grid system model is described by a family of continuous-time subsystems, called system configurations, each defined by a set of differential equations represented in state-space form. The dynamic model of each WECS configuration will depend on internal and external faults. The transition from the nominal (non-faulty) configuration to faulty configurations is random. For each of the possible configurations, the system dynamic performance

is evaluated to check whether or not certain WECS dynamic behavior meet some predefined performance requirements. A probabilistic measure that includes all operating conditions and all possible configurations that arise from faults can then be computed. The framework can be used for quantitative analysis of different WECS designs, including control strategies, and fault ride-through mechanisms. It can also be utilized to identify key parameters that affect WECS reliability, uncovering their relevance with respect to, for example, different grid codes. In order to illustrate certain features of the framework, we develop a case study for a doubly-fed induction generator (DFIG). In particular, we consider external faults in the grid and assume different operational scenarios arising from different wind speeds, fault duration times, voltage drops, and reactive power set-points.

The remainder of this paper is organized as follows. In Section II, we provide a detailed mathematical description of the framework building blocks. A case study of a doubly-fed induction generator (DFIG or type C WECS) illustrating the framework is presented in Section III. This section also includes a detailed description of a particular scenario dynamic simulation conducted in the case-study. Concluding remarks are discussed in Section IV. The case-study models are included in Appendix A.

II. FRAMEWORK MATHEMATICAL FORMULATION

This section describes the basic building blocks that comprise the proposed reliability analysis framework. For each building block, we provide a precise mathematical formulation and discuss how the overall framework can be implemented in a computer simulation environment. These building blocks, along with the exchange of information among them are illustrated in Fig. 1.

A. Framework Inputs

The reliability framework consists of four groups of inputs. The first three define WECS, grid, and faults characteristics. WECS characteristics feed the WECS model. Similarly, grid characteristics are an input for the grid model. Fault characteristics can feed both models. Within each of these groups, we can distinguish between i) model parameters, ii) deterministic input variables, and iii) random input variables.

For a particular WECS/grid system, model parameters are assumed to take constant values, and include for example, WECS rated power, WECS controller parameters, grid frequency, and grid nominal voltage at the interconnection point. Let $\{p_1, p_2, \dots, p_r\}$ denote the set of parameters, and define the corresponding parameter vector as $p = [p_1, p_2, \dots, p_r]'$.

Deterministic inputs are variables that govern the system dynamic evolution and are completely determined, e.g., WECS angular speed reference, and rotor-side converter current reference. We denote the set of deterministic inputs by $\{u_1, u_2, \dots, u_m\}$, and define the corresponding deterministic input vector as $u = [u_1, u_2, \dots, u_m]'$.

Random inputs are variables that govern the system dynamics over which we do not have control, and variables that are changed according to the operating conditions of the system to which the WECS is connected. These variables are described in probabilistic terms, as there is uncertainty associated with the values they take over time. Examples are wind speed and duration/ location of faults on the grid. Additionally, it is envisioned that WECS have the potential to provide reactive power support [18]. In this regard, the reactive power set-point of each turbine will be governed by the grid operating conditions, and thus it could be modeled as a random variable. If wind curtailment is to be considered, active power set-points could also be modeled as random variables as they will depend on the grid operating conditions. We denote by $\{w_1, w_2, \dots, w_s\}$ the set of random inputs, and define the corresponding random input variable vector as $w = [w_1, w_2, \dots, w_s]'$. Each input w_i is described by a random variable W_i with probability density function (pdf) denoted by $f_{W_i}(w_i)$. The joint pdf of $w = [w_1, w_2, \dots, w_s]'$ is denoted by $f_W(w_1, w_2, \dots, w_s)$, and takes values in some set $\mathcal{W} \in \mathbb{R}^s$. Random inputs can also be described as discrete random variables with a corresponding probability mass function (pmf). For the general discussion that follows, we consider they are continuous. In Section II-D we address this further.

Additionally, WECS internal and external faults are also assumed to occur randomly, causing abrupt changes in the WECS/grid system structure. For example, an external fault could be a short-circuit on the grid that causes a voltage drop on the WECS terminals. An internal fault could be caused by degradation in the rotor-side converter capacitor of a DFIG, or one of the power switches failing open circuit. We denote by k a variable that take values in a discrete set k_1, k_2, \dots, k_f that indexes all possible external and internal faults that cause changes in the system structure, as well as the nominal system configuration (no faults). The variable k is described by a random variable K with probability mass function (pmf) denoted by $p_K(k)$.

The fourth group of inputs is comprised of *performance requirements* that, for different operational scenarios, must be fulfilled by the WECS in the presence of internal and grid faults. These requirements consist of maximum and minimum values that certain WECS *performance variables* can take. As it will be discussed in the next section, performance variables usually describe WECS (dynamic) states, e.g., rotor current, or generator speed. For example, performance requirements can set a maximum value of the WECS rotor current. In this particular example, and given some operational scenario, the system will not fulfill its expected performance when the rotor current exceeds the maximum value defined by the performance requirements.

In general, we denote WECS performance variables by x_1, x_2, \dots, x_n and the corresponding performance variables vector by $x = [x_1, x_2, \dots, x_n]'$. The performance requirements will constrain the vector x to some region denoted by $\Phi \subseteq \mathbb{R}^n$. Thus, for a WECS to operate properly and fulfill its intended function, it is necessary that $x \in \Phi$ at all times. This definition of performance requirements and performance variables will naturally lead to the reliability measure definition proposed in Section II-C.

B. WECS and Grid Models

In general, the WECS model can range from a very simple relation between wind speed and output power, to a detailed model that captures electromechanical transients in the WECS generator. The level of detail is based on the objectives of the analysis. From a utility perspective, where numerous simulations for different grid conditions are needed in a planning study, simplified models might be the appropriate choice. For a wind turbine vendor, for whom it is important to precisely characterize WECS dynamic performance under all possible operational scenarios, including detailed dynamic models of each WECS component/subsystem is likely to be more appropriate. The grid can be described by a detailed model of a particular system where the WECS will be connected, or a standardized test model. Standard test models allow reliability comparisons between different WECS designs. WECS and grid models are connected by an interconnection sub-model, which is particularly important when these models use different reference frames.

In this work, we focus on the wind turbine manufacturer perspective, which is perhaps the level at which a WECS is modeled in most detail and the grid is described by a standard test model. Thus, the combined electromechanical WECS/grid model can be represented by a set of nonlinear differential equations (see, e.g., [19], [20]), described in state-space form as follows:

$$\frac{dx}{dt} = g_k(x, p, u, w), \quad (1)$$

where $x \in \mathbb{R}^n$ is the state-vector, $p \in \mathbb{R}^r$ is the vector of system deterministic parameters, $u \in \mathbb{R}^m$ is the vector of (possibly time-varying) inputs, $w \in \mathbb{R}^s$ is the vector of random inputs, $k \in \mathcal{K}$ indexes all possible internal and external faults, and $g_k(\cdot)$ governs the system dynamics evolution for every $k \in \mathcal{K}$.

As discussed in the previous section, the vector of random inputs is $W = [W_1, W_2, \dots, W_s]'$, where the W_i 's have a joint pdf denoted by $f_W(w_1, w_2, \dots, w_s)$. It is important to note that w are modeled as random variables and not as stochastic processes with some particular time structure. The difference is subtle but important. In this regard, once a fault occurs causing an abrupt change in (1), we are interested in quantifying whether or not the system survives the fault, hence, the focus is on the short-term behavior of (1) (in the order of seconds). Thus, even if W might include wind speed, which is bound to change over time, it is reasonable to assume that right after the fault, and in the timeframe of interest, wind speed does not significantly change. Thus, for each $k \in \mathcal{K}$, given the dependence of x on w as described in (1), x will also be described by a random vector denoted by $X = [X_1, X_2, \dots, X_n]'$, where the entries of X have a joint pdf denoted by $f_{X|k}(X_1, X_2, \dots, X_n)$.

C. Reliability Model

As stated before, for the WECS to properly fulfill its intended function, it is necessary that its performance variables are contained in the region defined by performance requirements, i.e., $x \in \Phi$ for all $t > 0$, otherwise it is considered as failed. Then, since the performance variables x are described by a random vector X , a natural way to define WECS reliability is the probability that the performance variables x will remain within the region defined by Φ at all times. Thus, for every $k \in \mathcal{K}$, we define WECS reliability as

$$\begin{aligned} R_k &= \Pr\{X \in \Phi | K = k\} \\ &= \int_{\Phi} f_{X|k}(x_1, x_2, \dots, x_n) dx_1 dx_2 \dots dx_n. \end{aligned} \quad (2)$$

It is evident that for nominal system configuration (no faults), which can be denoted by $k = 0$, $R_{K=0} = 1$.

By using the total probability theorem, it is possible to define a global measure of WECS reliability that encompasses all possible faults indexed by \mathcal{K} and also stochastic phenomena driving the system dynamics described in W . Let R denote WECS overall measure of reliability, then

$$R = \sum_{k \in \mathcal{K}} R_k \Pr\{K = k\}, \quad (3)$$

where for each k , R_k can be obtained using (2).

It is clear that in order to compute (2) (and therefore (3)), it is necessary to obtain $f_{X|k}(x_1, x_2, \dots, x_n)$ ($\Pr\{K = k\}$ is known since $p_K(k)$ is part of the input data). In order to obtain $f_{X|k}(X_1, X_2, \dots, X_n)$, it is necessary to first obtain the functional relation between x and w . This functional relation, denoted by $x(t) = G_k(w, t)$, can be obtained by solving the differential equation in (1) ($G_k(\cdot)$ is assumed to include the dependence of x on p , u , and $x(0)$). Then, the pdf of the random variable X can be computed by using the method of random variable transformations (see, e.g., [21]), as a function of $f_W(w_1, w_2, \dots, w_s)$ and the Jacobian of the mapping between w and x , which in theory can be obtained by inverting the functional relation $G_k(\cdot)$. For linear systems, a complete discussion of the ideas discussed above can be

found in [22]. However, for general nonlinear systems, the above random variable transformation procedure is challenging. Thus, in order to circumvent the problem, instead of defining the reliability measure R in the performance-variable space, it is possible to define it in the input space as follows. Let $\overline{\mathcal{D}}_k := G_k^{-1}(\Phi, t)$, then R_k can be obtained as

$$\begin{aligned} R_k &= \Pr\{X \in \Phi | K = k\} = \Pr\{G_k(W, t) \in \Phi\} \\ &= \Pr\{W \in G_k^{-1}(\Phi, t)\} = \Pr\{W \in \overline{\mathcal{D}}_k\} \\ &= \int_{\overline{\mathcal{D}}_k} f_W(w_1, w_2, \dots, w_s) dw_1 dw_2 \dots dw_s. \end{aligned} \quad (4)$$

The set $\overline{\mathcal{D}}_k \subseteq \mathbb{R}^s$ is the region of the space where W is defined, such that if $W \in \overline{\mathcal{D}}_k$, then it follows that $x \in \Phi$ for all $t > 0$. Sometimes, it is more convenient to define (4) in terms of the complement of $\overline{\mathcal{D}}_k$, denoted by \mathcal{D}_k , as follows:

$$\begin{aligned} R_k &= 1 - \Pr\{W \in \mathcal{D}_k\} \\ &= 1 - \int_{\mathcal{D}_k} f_W(w_1, w_2, \dots, w_s) dw_1 dw_2 \dots dw_s. \end{aligned} \quad (5)$$

The set $\mathcal{D}_k \subseteq \mathbb{R}^s$ can be interpreted as the region of the W -space, such that if $w \in \mathcal{D}_k$, then at least one of the performance variables will exceed its requirements.

D. Computer Implementation Details

In the context of WECS, obtaining analytically tractable solutions for (1)–(5) is not possible in general. In both (4) and (5), $f_W(\cdot)$ is known, and the challenge is to obtain $\overline{\mathcal{D}}_k$ and \mathcal{D}_k , which results from mapping Φ and its complement $\overline{\Phi}$ into the input space through $G_k^{-1}(\cdot)$. Thus, a simulation environment is needed to develop the framework. First, it is necessary to implement the WECS/grid dynamic model described in (1), which can be accomplished with a simulation package like MATLAB/Simulink. Once the simulation model has been constructed, there are two ways to calculate R_k and R .

1) *Scenario enumeration*: The first approach to compute R , which is the one used in the case study presented in Section III, relies on discretizing each W_1, W_2, \dots, W_s into $N_{W_1}, N_{W_2}, \dots, N_{W_s}$ values, respectively. In practice, the distributions of W_1, W_2, \dots, W_s are usually obtained from empirical data, e.g., wind speed, and therefore, it is more natural to actually describe them as discrete¹ random variables, obtaining their joint pmf directly from the data (see, e.g., [24]). Thus, let $p_W(w_1, w_2, \dots, w_s)$ denote the joint pmf of W_1, W_2, \dots, W_s , taking $N_{W_1} \times N_{W_2} \times \dots \times N_{W_s}$ values. Then, for a particular fault k , and for each realization of the discretized W , the response of the system, described by (1) is simulated. If $x(t) \notin \Phi$, for some $t > 0$, for the particular realization of W , the system is declared as failed. Then, it is possible to obtain an estimate of R_k as follows:

$$\begin{aligned} R_k &= 1 - \Pr\{W \in \mathcal{D}_k\} \\ &= 1 - \sum_{w \in \mathcal{D}_k} p_W(w_1, w_2, \dots, w_s), \end{aligned} \quad (6)$$

¹In the context of power system reliability analysis, even if there are certain variables such as daily loads that are described by continuous random variables, it is common to assume they take discrete values, e.g., two-level and multi-level models [23], and describe them as discrete random variables.

where $p_W(\cdot)$ is the discrete counterpart of $f_W(\cdot)$, and \mathcal{D}_k (the discrete counterpart of \mathcal{D}_k in (5)) is the set that contains all possible realizations of W that result in system failure. Computing the overall reliability measure R is straightforward using (3), since the pmf of K is known.

2) *Stochastic simulation*: The second approach, also referred to as Monte Carlo simulation [25], is in the vein of stochastic simulation techniques used in power system reliability analysis (see e.g., [23]). In this approach, $f_W(w_1, w_2, \dots, w_n)$ and $p_K(k)$ are repeatedly sampled, and for each sample $(w_1, w_2, \dots, w_n, k)$, the response of the system is simulated. Then, if $x(t) \notin \Phi$, for some $t > 0$, for the particular sample $(w_1, w_2, \dots, w_n, k)$, the system is declared as failed. Let N denote the total number of simulations and F the total number of simulations that results in system failure, then the overall reliability measure can be obtained as $R = 1 - F/N$. For a more detailed discussion on the theory of stochastic simulation the reader is referred to [25].

The utilization of one approach or the other depends on the nature of the problem. If the number of random variables W is very large, then the scenario enumeration approach might be prohibitive, and the stochastic simulation approach might be better suited. On the other hand, if the number of random variables W is small, then the number of scenarios that result from discretizing W might be small enough to justify the scenario enumeration approach. If done correctly, both approaches should yield similar results. In the context of power system reliability analysis, additional discussion on the tradeoffs between both approaches can be found in [23].

III. TYPE C WECS RELIABILITY ANALYSIS CASE STUDY

In this section, the proposed framework is used to analyze the reliability of a DFIG. Although, the framework can include both internal and external faults, we only address external (grid) faults. In order to include internal faults in the analysis, it is necessary to have detailed proprietary models of each WECS component, which were not available to the authors at the time this work was completed. A discussion on how internal faults could be incorporated in the analysis is included.

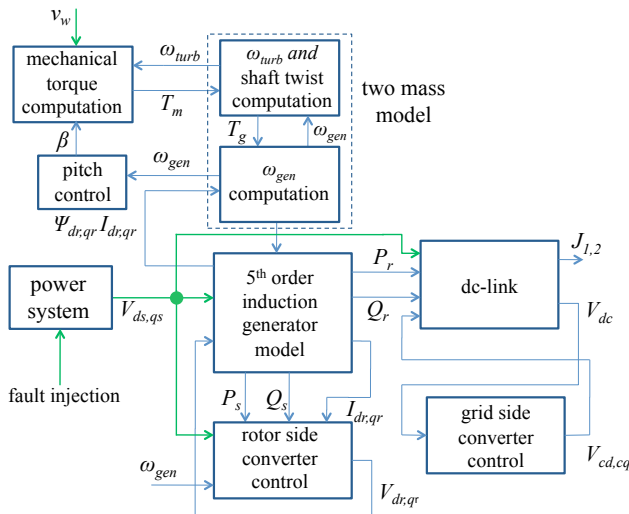


Fig. 2. DFIG/Grid dynamic model block diagram.

A. WECS and Grid Models

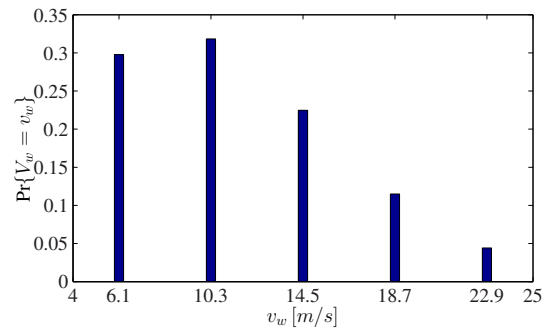
A detailed DFIG simulation-based dynamic model was developed in MATLAB/Simulink, the block diagram of which is shown in Fig. 2. The model elements are: i) mechanical torque, ii) two mass turbine, iii) 5th-order induction generator, iv) rotor side converter (RSC) control, v) pitch control, vi) dc-link, and vii) grid side converter (GSC) control. Most of these models are adopted from [19], [20], and are included in Appendix A for completion.

The main elements of the grid model consist of a voltage source with its corresponding source impedance, a π model for the line connecting the WECS with the system, and the transformer. The main parameters of our grid model are system voltage level V_{sys} , with the corresponding angle $V_{sys\ angle}$; grid frequency f ; system source impedance Z_{sys} ; source impedance ratio R/X ; and line and transformer impedances.

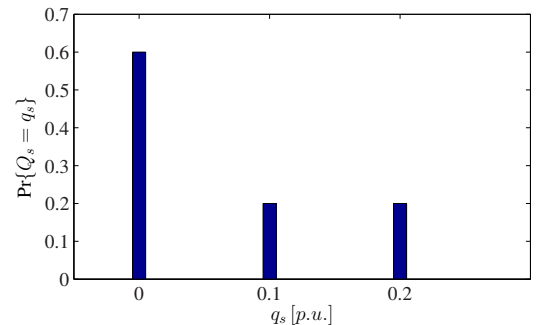
All grid model parameters are assumed to be deterministic. There might be cases where some of those parameters are described as random variables. For example, the system voltage or the system source impedance could take different values, capturing the uncertainty in operating conditions that would arise if this simplified model represented the grid.

B. Inputs

The group of parameters and deterministic inputs includes rated power; cut-in, cut-off and rated wind speed; and maximum and minimal generator angular speed. A complete list of parameters and deterministic inputs is given in Appendix B. As shown in Fig. 3, wind speed v_w , and the set value of reactive power generation q_s are described by a probabilistic model, where the corresponding random variables describing v_w and q_s are denoted by V_w and Q_s , respectively.



(a) Wind speed V_w pdf.



(b) Reactive power generation set point Q_s pdf.

Fig. 3. Wind speed and reactive power generation set point pdfs.

The assumption of just one wind speed for assessing reliability would lead to results with limited significance. For example, using a low wind speed may leave higher current reserves, such that rotor transients may not violate the limit or activate protections, whereas operating close to the rated wind speed may result in protection activation, which would eventually cause the turbine to shut down. In this example, the wind speed is assumed to be Rayleigh distributed, with an average of 8.6 m/s. This distribution is discretized to five values as shown in Fig. 3(a). Wind speeds below $v_{cut-in} = 4$ m/s and above $v_{cut-off} = 25$ m/s are not taken into account, and the pdf is normalized such that $\sum_{v_w} \Pr\{V_w = v_w\} = 1$.

Reactive-power set points are not usually described by a random variable, as they are set by the turbine manufacturer or by the grid operator. Their value depends on grid code and operator policy, which does not necessarily result in a constant q_s value. For example, a grid operator who wants to cover his reactive power deficit, might increase the q_s value on wind farms in his system. Obtaining the pdf for q_s might be a difficult task, and requires data of system operator activity. The reactive power set point probability distribution used in this case-study is shown in Fig. 3(b), where the pdf probabilities are based on the assumption that this WECS operates 60% of the time close to zero reactive power exchange.

Voltage drop value v_{drop} , and fault duration t_{fault} are described by random variables, denoted by V_{drop} and T_{fault} respectively. Voltage drop is the per unitized difference of the positive-sequence voltage root-mean-square value before the voltage dip and during the dip (neglecting transient flickering). Fault duration is the period between the fault occurrence and the fault clearance. Fault characteristics are based on EPRI data [26], from where we conclude that fault duration and voltage drop are not independent variables and therefore they must be described by their joint pdf as shown in Fig. 4.

Since only faults in the grid are being considered, and we model them by a change (of different value) in the voltage on the WECS terminals, the discrete variable k that indexes all possible WECS/grid configurations (fault/non-faulty) as described in (1), only takes two values: $k = 0$, which indexes the nominal non-faulty dynamics, and $k = 1$, which indexes the dynamics after a fault in the grid. If internal faults were to be included, then this would result in additional k 's and their corresponding configurations as described in (1).

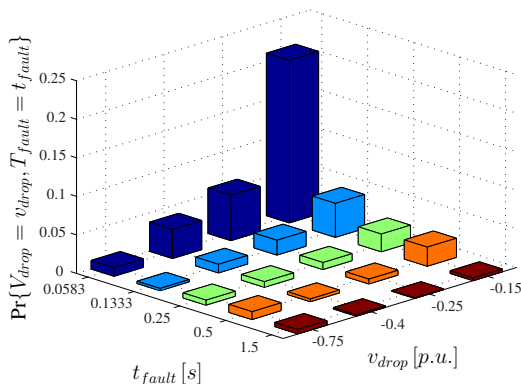


Fig. 4. Fault duration t_{fault} and voltage drop V_{drop} joint pmf.

Performance requirements for WECS are mainly concerned with LVRT. Other requirements that wind farms must fulfill include: active power regulation, reactive power regulation, voltage quality (harmonics, flickering), and steady-state power production depending on voltage and frequency level. For simplicity, the performance requirements specify that the current in the rotor circuits should not exceed the value of $1.5I_{r,n}$, where $I_{r,n}$ is the rotor nominal current. It is assumed that this current would block the converters, leading to turbine shutdown. After defining performance requirements, dynamic simulations are conducted. Each simulation violating requirements is declared as failed.

C. Reliability Assessment

In order to conduct the reliability assessment, we will follow the scenario enumeration procedure described in Section II-D. There are only four random inputs, i.e., wind speed V_w with pmf $p_{V_w}(v_w)$, reactive power set-point Q_s with pmf $p_{Q_s}(q_s)$, fault duration T_{fault} , and voltage drop during the fault V_{drop} , with joint pmf $p_{V_{drop}, T_{fault}}(v_{drop}, t_{fault})$. Although V_{drop} and T_{fault} are not independent, it is assumed they are jointly independent of V_w and Q_s . Therefore, the joint pmf of $W = [V_w, Q_s, V_{drop}, T_{fault}]'$ is given by

$$p_W(v_w, q_s, v_{drop}, t_{fault}) = p_{V_w}(v_w) \times p_{Q_s}(q_s) \times p_{V_{drop}, T_{fault}}(v_{drop}, t_{fault}). \quad (7)$$

Since V_w can take 5 different values; Q_s can take 3; and V_w and Q_s jointly take 20, the number of scenarios is $5 \times 3 \times 20 = 300$. For each scenario, a dynamic simulation (see details in Section III-E for details) is conducted. The ones declared as a failure will be used for computing $R_{K=1}$, which is the reliability of the WECS given a fault in the grid. The subsequent analysis focuses on $R_{K=1}$ and how it could be improved by modifying certain design parameters.

As shown in Table I, the overall reliability measure is 0.8685. In order to improve reliability, some modifications in WECS control or design can be introduced. For example, if the rotor inductance X_r and resistance R_r are increased by 30%, the new reliability measure is 0.8852. However, an increase in those parameters can also increase steady-state power losses. Also, for this particular example, and as shown in Table II, the stronger the grid, the easier it is to fulfill requirements.

TABLE I
 $R_{K=1}$ AS A FUNCTION OF ROTOR RESISTANCE AND REACTANCE.

R_r [p.u.]	X_r [p.u.]	$R_{K=1}$
0.005	0.2	0.8685
0.00575	0.23	0.8746
0.0065	0.26	0.8852

TABLE II
 $R_{K=1}$ AS A FUNCTION OF SYSTEM SHORT-CIRCUIT POWER.

$S_{sys\ sc}$ [VA]	$R_{K=1}$
$0.5 \cdot 10^7$	0.8441
10^7	0.8685
$2 \cdot 10^7$	0.9193

TABLE III

 $R_{K=1}$ AS A FUNCTION OF ACTIVE POWER PI CONTROLLERS GAINS.

$k_{p,P}$	$k_{i,P}$	$k_{p,I}$	$k_{i,I}$	$k_{p,\omega}$	$k_{i,\omega}$	$R_{K=1}$
0.112	0.37	0.54	0	5	0	0.8685
0.14	0.463	0.675	0	6.25	0	0.8765
0.186	0.555	0.81	0	7.5	0	0.8764

TABLE IV

 $R_{K=1}$ AS A FUNCTION OF SYSTEM SHORT-CIRCUIT POWER AND ROTOR RESISTANCE AND REACTANCE.

R_r [p.u.]	X_r [p.u.]	$S_{sys\ sc}$ [VA]	$R_{K=1}$	$\Delta R_{K=1}$
0.005	0.2	10^7	0.8685	0%
0.0065	0.26	10^7	0.8852	1.92%
0.005	0.2	$2 \cdot 10^7$	0.9193	0%
0.0065	0.26	$2 \cdot 10^7$	0.9281	0.96%

TABLE V

 $R_{K=1}$ AS A FUNCTION OF THE SYSTEM SHORT-CIRCUIT POWER AND THE ACTIVE POWER PI CONTROLLERS GAINS.

$S_{sys\ sc}$	$k_{p,P}$	$k_{i,P}$	$k_{p,I}$	$k_{p,\omega}$	$R_{K=1}$	$\Delta R_{K=1}$
10^7	0.112	0.37	0.54	5	0.8685	0%
10^7	0.14	0.463	0.675	6.25	0.8765	0.92%
10^7	0.186	0.555	0.81	7.5	0.8764	0.91%
$2 \cdot 10^7$	0.112	0.37	0.54	5	0.9193	0%
$2 \cdot 10^7$	0.14	0.463	0.675	6.25	0.9083	-1.2%
$2 \cdot 10^7$	0.186	0.555	0.81	7.5	0.9046	-1.6%

Another set of WECS parameters that affect reliability are active and reactive power control gains. The issue of setting correct PID gains is broad enough to warrant a separate study. Additionally, gain values will change for different control objectives, such as minimization of rotor shaft oscillations or rotor current transients. Table III presents the reliability assessment results for three gain sets. The gains increase leads to an increase in WECS reliability. In order to find the best set of values that fulfill the particular performance requirements, a multi-variable optimization process based on the proposed reliability framework could be carried out.

The proposed framework identifies key parameters that affect WECS reliability and ascertains their significance with respect to different WECS and grid characteristics. For instance, the results in Table IV demonstrate that a 30% increase in rotor circuit impedance in a system with 10^7 VA short-circuit power gives a 1.92% increase in WECS reliability. A similar analysis can be performed with respect to the system short-circuit power and the active power PI controller gains (see Table V). For the 10^7 VA system, the 25% and 50% PI gains change produce, respectively, a 1.92% and a 0.91% $R_{K=1}$ increase; whereas for the $2 \cdot 10^7$ VA system, the same controller gains increase result in a -1.2% and a -1.6% R_w decrease.

D. Including WECS internal faults

Modeling WECS internal faults requires detailed models of the components within the WECS. The availability of these models in the open literature is limited. Although not included in the case study discussed above due to lack of accurate models, we illustrate with a simple example how the effect of WECS internal faults can be naturally captured by the proposed framework.

Consider for example an encoder for measuring the speed of WECS electric generator. This is one of the components utilized in the WECS active power control loop and also in the pitch angle control loop. A failure of such a sensor can cause a degradation of WECS dynamic performance. We describe next how to model internal faults in the dynamic model of such a component. Let ω_g denote the WECS generator speed, and let y_g be the measurement provided by the encoder. Assume for simplicity that the sensor input/output transfer function can be described by a constant gain G . Assume that the encoder is subject to internal faults that results in one of the following: i) the encoder gain changes by a quantity ΔG , or ii) the encoder output measurement is biased by a fixed quantity B . Let $K_s = \{0, 1, 2\}$ describe the sensor failure status. Then a simple sensor model describing both its nominal (non-faulty) and fault behavior is given by

$$y_g = \begin{cases} G\omega_g, & \text{if } K_s = 0, \\ (G + \Delta G)\omega_g, & \text{if } K_s = 1, \\ G\omega_g + B, & \text{if } K_s = 2, \end{cases} \quad (8)$$

Incorporating such a model in a simulation model is not a difficult task as discussed in [27]. In the context of the general model described in (1), incorporating such a fault model adds three new configurations besides the nominal non-faulty one. In the context of our case-study, in order to calculate R_k for each of this particular encoder faults, it would be necessary to evaluate WECS performance for each pair of wind speed value and reactive power set-point values. Note that, since fault duration and voltage drop are associated with grid faults, they are not considered in the analysis of encoder faults.

E. Dynamic Simulation Analysis for a Particular Scenario

This section demonstrates an example of a dynamic simulation associated with a particular scenario conducted during the reliability analysis. The impact of the fault on relevant WECS variables is discussed in detail. The scenario described in this particular simulation is defined by: i) wind speed during simulation: $V_w = 14$ m/s; ii) reactive power set-point: $Q_s = 0.1$ p.u.; iii) voltage drop during fault: $V_{drop} = 40\%$; and vi) fault duration: $T_{fault} = 300$ ms. Motor conventions are used, e.g., generated power is negative.

1) *Stator and rotor currents:* As shown in Fig. 5, rotor current I_{dr} reaches its maximum value immediately after the fault is cleared, which can cause the turbine to trip. This phenomenon is mostly caused by reactive and active current control, which sets current and power values during the fault by changing the RSC voltage (there is no LVRT control mechanism).

2) *Reactive power:* Reactive power exchange at the GSC terminals is caused directly by the voltage drop. After the fault, the GSC control brings P_c to its set point by altering the GSC voltage. Unfortunately, that change of voltage $V_{cd,cq}$ leads to an overshoot when the fault is removed and the grid voltage returns to its pre-fault value. As seen in Fig. 6, stator and rotor reactive powers oscillate in the vicinity of their steady-state values ($Q_{s\ set} = 0.1$ p.u., $Q_{c\ set} = 0$ p.u.).

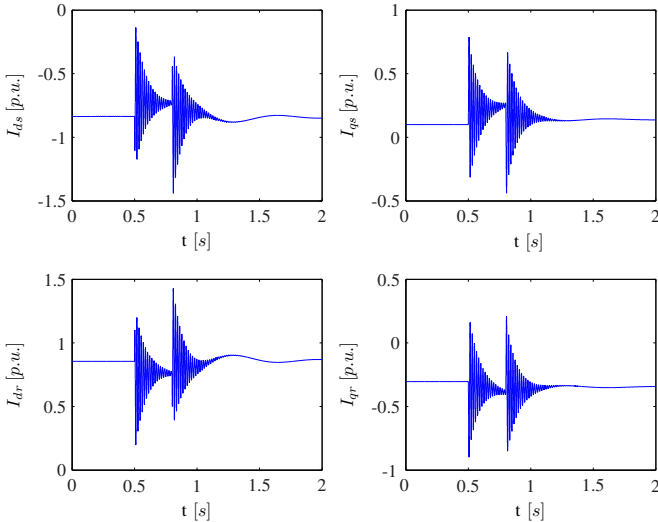


Fig. 5. Stator and rotor currents in $dq0$ axis.

3) *Electrical and mechanical torques*: The sudden stator voltage decrease during the fault creates a situation in which the WECS cannot export the energy produced to the grid. This can be seen in Fig. 7 by tracing the value of the electrical torque T_e , which oscillates in the vicinity of 0.453 (smaller value than before the fault). This results in an imbalance between the mechanical torque generated by the wind ($T_{m,t}$, $T_{m,r}$) and the generator electrical torque (T_e), which leads to an increase in the rotor (and turbine) angular speed.

IV. CONCLUDING REMARKS

In this paper, we introduced a framework for WECS reliability and dynamic performance evaluation. The framework includes all possible operating conditions that the WECS might be subject to, and also all possible internal and external faults that might affect WECS performance. For example, for every particular internal and external fault, it can take into account all possible wind speeds the WECS will be subject to, or all possible active and reactive power commands. In this regard, the effect of wind curtailment on overall WECS

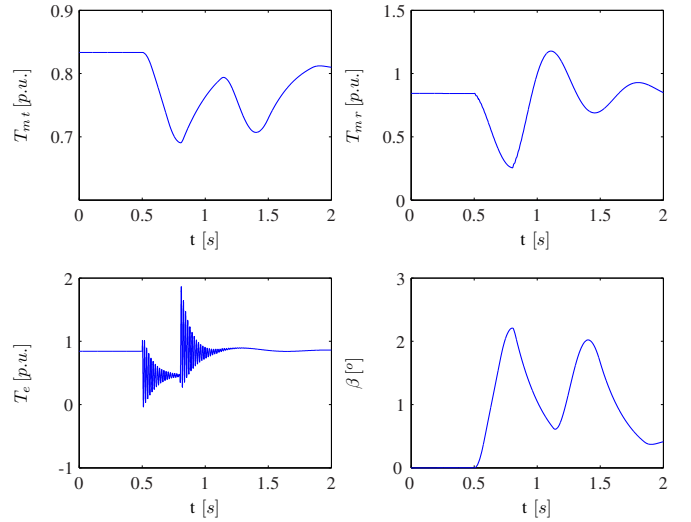


Fig. 7. Turbine mechanical torque, rotor mechanical torque, electrical torque and pitch angle.

reliability can be easily assessed by describing the active power command as a random variable, the distribution of which depends on the grid operational policies to which the WECS is connected. As WECS and other distributed energy resources are forced to provide reactive power support, it is also possible to include the effect of different reactive power set-points on WECS reliability. The framework can include other variables that might not be completely known as they depend on the grid location, e.g., fault duration, voltage drop, and short circuit power.

The application of the framework was illustrated with a case study, where we calculated WECS reliability for grid faults, including different wind speed scenarios, reactive power set-points, different fault duration times, and also different voltage drops in the WECS terminals. The scope of this case study is thus limited and it does not describe the full power of the proposed framework, as it does not consider the effect of WECS internal faults. These limitations are due to the lack of the appropriate individual WECS components for including the effect of faults available in the open literature. However, if appropriate models are available to the end user of this framework, including them in the analysis should be an amenable task as described in Section III-D.

Although not discussed in the paper, the proposed framework can be used to obtain availability models for power system reliability analysis. For example, in (1), one of the configurations can correspond to a situation in which the WECS is forced out, and thus a transition to such configuration contributes to the unavailability probability. In this regard, the proposed overall measure of reliability can be interpreted as the availability of an individual WECS, similar to the availability numbers used for conventional generating units in power system reliability analysis. Thus, we envision that for a particular wind power plant, the individual WECS reliability measures as calculated in detail using the proposed framework could be integrated to obtain the overall availability of the particular wind power plant. This is a topic of further research.

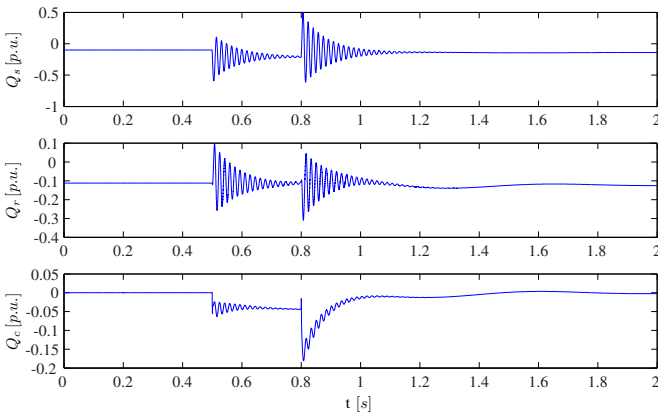


Fig. 6. Stator reactive power Q_s , rotor reactive power Q_r , grid side converter reactive power Q_c (motor convention).

APPENDIX

A. Case-Study Models

1) *Mechanical torque [19]*: Mechanical power is given by

$$P_m = \frac{1}{2} \rho \pi R^2 C_p(V, \beta, \omega_{turb}) V_w^3, \quad (9)$$

where ω_{turb} is the turbine angular speed, β is the pitch angle, V_w is the wind speed, ρ is the air density, R is the radius of the area covered by the wind turbine, and C_p is the power coefficient, which is defined as:

$$C_p = c_1 \left(\frac{c_2}{\lambda_i} - c_3 \beta - c_4 \beta^{c_5} - c_6 \right) e^{-\frac{c_7}{\lambda_i}},$$

$$\lambda_i = \left[\frac{1}{\lambda + c_8 \beta} - \frac{c_9}{\beta^3 + 1} \right]^{-1}, \quad \lambda = \frac{\omega_{turb} R}{V_w} \quad (10)$$

λ is the tip-speed ratio. The mechanical torque of the turbine shaft can be computed by

$$T_m = \frac{P_m}{\omega_{turb}}. \quad (11)$$

2) *Two-mass system [19]*: The turbine angular speed is defined by:

$$2H_t \frac{d\omega_{turb pu}}{dt} = T_m pu - D(\omega_{turb pu} - \omega_{rotor pu}) - K_s \theta, \quad (12)$$

where H_t is the turbine inertia, D is the damping coefficient, K_s is the shaft stiffness, and θ is the angle of shaft twist in radians. The generator rotor angular speed is governed by

$$2H_g \frac{d\omega_{rotor pu}}{dt} = D(\omega_{turb pu} - \omega_{rotor pu}) + K_s \theta - T_e, \quad (13)$$

where H_g is the generator inertia, T_e is the per-unit electrical torque of the generator. Shaft twist angle between turbine mass and rotor mass is governed by

$$\frac{d\theta}{dt} = (\omega_{turb pu} - \omega_{rotor pu}) \omega_{base rps}, \quad (14)$$

where $\omega_{base rps}$ is the base angular speed in radians per second.

3) *Fifth-order induction generator model [20]*: The induction machine is described by a fifth-order differential equation in the $dq0$ reference frame with per-unit variables:

$$V_{ds} = R_s I_{ds} - \Psi_{qs} + \frac{1}{\omega_{base rps}} \frac{d\Psi_{ds}}{dt},$$

$$V_{qs} = R_s I_{qs} + \Psi_{ds} + \frac{1}{\omega_{base rps}} \frac{d\Psi_{qs}}{dt},$$

$$V_{dr} = R_r I_{dr} - \frac{1}{\omega_{base rps}} \frac{d\theta_r}{dt} \Psi_{qr} + \frac{1}{\omega_{base rps}} \frac{d\Psi_{dr}}{dt},$$

$$V_{qr} = R_r I_{qr} + \frac{1}{\omega_{base rps}} \frac{d\theta_r}{dt} \Psi_{dr} + \frac{1}{\omega_{base rps}} \frac{d\Psi_{qr}}{dt},$$

$$\frac{d\theta_r}{dt} = \omega_{e rps} - \omega_{gen rps}, \quad (15)$$

where $V_{ds,qs}$ are stator voltages in the $dq0$ axis, $V_{dr,qr}$ are rotor voltages, $I_{ds,qs}$ stator currents, $I_{dr,qr}$ rotor currents, $\Psi_{ds,qs,dr,qr}$ are respectively stator and rotor fluxes, $R_{s,r}$ are stator and rotor circuit resistances respectively, and $\omega_{e rps}$ is the grid electrical-field pulsation (usually equal to $\omega_{base rps}$).

The relations between fluxes and currents are given by:

$$\Psi_{ds} = (X_s + X_m) I_{ds} + X_m I_{dr},$$

$$\Psi_{qs} = (X_s + X_m) I_{qs} + X_m I_{qr},$$

$$\Psi_{dr} = (X_r + X_m) I_{dr} + X_m I_{ds},$$

$$\Psi_{qr} = (X_r + X_m) I_{qr} + X_m I_{qs}, \quad (16)$$

where $X_{s,r}$ are stator and rotor circuit reactances, and X_m is the magnetizing reactance, all in per unit values (p.u.).

The machine electrical torque is given by:

$$T_e = \Psi_{qr} I_{dr} - \Psi_{dr} I_{qr}. \quad (17)$$

4) *Rotor-side converter (RSC) control [20]*: RSC control is based on two PI sets. The first set controls the active power and the second, the reactive power. Active power control consists primarily of three PI controllers. The first one controls the value of I_{qr} by changing V_{qr} and the second tries to keep the stator power P_s equal to its set value $P_{s set}$ by influencing the set value of current $I_{qr set}$. The third controller used in the active power set has the goal of damping the turbine and rotor angular speed oscillations.

Reactive power control consists of three PI controllers. The first one controls the value of I_{dr} by changing V_{dr} . This PI controller (like the corresponding controller for active power) does not have integral part $k_i I_{dr} = 0$ ($k_i I_{qr} = 0$); thus, proportional gain is greater than the reactive (and active) power controller, $k_p I_{dr} > k_p Q_s$ ($k_p I_{qr} > k_p P_s$). The last controller tracks the stator voltage magnitude, V_s , error by changing the set value of reactive power $Q_{s set}$.

5) *Pitch control [19]*: The pitch control system inputs are ω_{gen} and the initial pitch angle, β_0 . The element in the pitch control that simulates the mechanical blades motion is an integrator. The gain, $1/T_{servo}$, represents the delay of the servomotors rotating the blades; the value of T_{servo} is usually equal to a fraction of a second. The description of blade motion needs to have limitations in terms of a minimum and maximum value of the pitch angle β and its change, $d\beta$.

6) *Direct-current link model [20]*: The capacitor voltage in the dc-link between the RSC and the GSC is given by:

$$\frac{dV_{DC pu}}{dt} = \frac{1}{C} (P_{gsc} - P_r), \quad (18)$$

where P_{gsc} is the active power flowing between GSC and the dc-link, C is the dc-link capacitor capacity, and P_r is the active power between RSC and the dc-link defined as:

$$P_r = V_{dr} I_{dr} + V_{qr} I_{qr}. \quad (19)$$

If losses in the dc-link are neglected, $P_r = P_{gsc}$. Assuming that $R_c \approx 0$, active power flowing through GSC is equal to the active power at the GSC terminal, P_c , and thus

$$P_c = V_{ds} I_{cd} + V_{qs} I_{cq}, \quad (20)$$

where $V_{ds,qs}$ are the $dq0$ stator voltage components, and $I_{cd,cq}$ are the $dq0$ components of the current flowing into the grid.

7) *Grid side converter (GSC) control [20]*: GSC control consists of two sets of PI controllers. The first one is based on active current, I_{cd} , control. For this set, the values which

are being controlled by the change of GSC voltage component V_{cd} , are the dc-link capacitor voltage, V_{DC} , and the GSC active current, I_{cd} . The second set consists of one PI controller that reacts to changes in I_{cq} by changing V_{cq} .

8) *Grid model*: The grid model used in this study consists of a voltage source and a source impedance that represent the grid from the WECS perspective, together with a π model of a line connecting the WECS with the system and the transformer. The WECS model is based on the $dq0$ axis, while the grid model is a three-phase abc system. For this reason, it is necessary to include $dq0$ - abc and abc - $dq0$ transformations.

B. Case-Study Parameters and Variables Values

1) *WECS parameters and variables*: nominal power, $P_n = 2 \cdot 10^6$ W; nominal wind speed, $V_{wn} = 14$ m/s; cut-in wind speed, $V_{w\ cut\ in} = 4$ m/s; cut-off wind speed, $V_{w\ cut\ off} = 25$ m/s; air density, $\rho = 1.25$ kg/m³; $\omega_{gn\ pu} = 1.2$; $\omega_{gn\ pu} = 0.5$; number of poles, $P = 4$; steady-state pitch angle control coefficient, $K_b = 2.19$; nominal voltage on WECS terminals, $V_{wecs\ pu} = 1$; power curves coefficients, $c_1 = 0.73$, $c_2 = 151$, $c_3 = 0.58$, $c_4 = 0.002$, $c_5 = 2.14$, $c_6 = 13.2$, $c_7 = 18.4$, $c_8 = -0.02$, $c_9 = -0.003$; stator resistance, $R_s = 0.01$ p.u.; stator reactance, $X_s = 0.12$ p.u.; mutual reactance, $X_m = 5$ p.u.; rotor resistance, $R_r = 0.005$ p.u., rotor reactance, $X_r = 0.2$ p.u., resistance between GSC and WECS grid terminals, $R_c = 0.0001$ p.u., reactance between GSC and WECS grid terminals (mainly from smoothing inductor), $X_c = 0.3$ p.u.; the dc-link capacitor capacity, $C = 6 \cdot 10000 \cdot 10^{-6}$ F; generator inertia, $H_g = 0.7$ s; turbine inertia, $H_t = 5$ s; damping coefficient, $D = 0.01$ p.u.; stiffness coefficient, $K_s = 0.3$ p.u./el.rad; active power control PI gains: $k_{pP} = 0.112$; $k_{iP} = 0.37$; $k_{pI} = 0.54$; $k_{iI} = 0$; $k_{p\omega} = 5$; $k_{i\omega} = 0$; reactive power control PI gains: $k_{pQ} = 0.004$; $k_{iQ} = 0.015$; $k_{pI} = 0.54$; $k_{iI} = 0$; $k_{pV} = k_{pQ}$; $k_{iV} = k_{iQ}$; grid side converter PI gains: $k_{pI} = 0.54$; $k_{iI} = 0$; $k_{pVdc} = k_{pI2} = k_{pI}$; $k_{iVdc} = k_{iI2} = k_{iI}$; pitch angle control coefficients: $K_p = 175$; $\beta_{max} = 60$ deg; $\beta_{min} = 0$ deg; $\frac{d\beta}{dt\ max} = 10$ deg/s; $\frac{d\beta}{dt\ min} = -10$ deg/s; $T_{servo} = 0.25$ s;

2) *Grid parameters and variables*: grid frequency $f = 60$ Hz; grid pulsation, $\omega_{erps} = 2\pi f$; system source voltage, $V_{sys} = 25 \cdot 10^3$ V; system source voltage angle, $V_{sys\ angle} = 0$ deg; systems short-circuit power, $S_{sys\ sc} = 10^6$ VA; system impedance ratio, $\frac{X}{R}_{sys} = 10$; system source-transformer line parameters: $l_{km} = 10$, $R_1 = 0.1153$ Ω /km, $R_0 = 0.413$ Ω /km, $L_1 = 1.05 \cdot 10^{-3}$ H/km, $L_0 = 3.32 \cdot 10^{-3}$ H/km, $C_1 = 11.33 \cdot 10^{-9}$ F/km, $C_0 = 5.01 \cdot 10^{-9}$ F/km; transformer parameters: $P_{nt} = 1.5 \cdot P_n$, $V_t = 575$ V, $L_{winding\ 1\ pu} = 0.025$, $R_{winding\ 1\ pu} = L_{winding\ 1\ pu}/30$, $L_{winding\ 2\ pu} = 0.025$, $R_{winding\ 2\ pu} = L_{winding\ 2\ pu}/30$, $R_{m\ pu} = 500$;

3) *Simulation parameters*: fault start, $t_{fault\ start} = 0.2$; fault clearing, $t_{fault\ cleared} = 0.3$; base power, $P_b = P_n$; base WECS voltage, $V_b = 575$ V; base WECS phase-to-ground voltage, $V_{b\ ph-g} = V_b/\sqrt{3}$; base current, $I_b = P_b/(3V_{b\ ph-g})$; base impedance, $Z_b = V_{b\ ph-g}/I_b$; base system voltage, $V_{sys\ b} = V_{sys}$; simulation step size, $h = 50 \cdot 10^{-6}$ s; pitch angle control step size, $T_s = h$; PI controllers step size, $h_{pI} = h$.

REFERENCES

- [1] "20% of wind energy by 2030: Increasing wind energy's contribution to U.S. electricity supply," U.S. Department of Energy, Washington, DC, Tech. Rep. DOE/GO-102008-2567, 2006.
- [2] I. Erlich and H. Brakelmann, "Integration of wind power into the german high voltage transmission grid," in *Proc. of IEEE PES GM*, June 2007.
- [3] S. Smater and A. Domínguez-García, "A Unified Framework for Reliability Assessment of Wind Energy Conversion Systems," in *Proc. of IEEE PES General Meeting*, July 2010.
- [4] E. Gavanidou, A. Bakirtzis, and P. Dokopoulos, "A probabilistic method for the evaluation of the performance of wind-diesel energy systems," *IEEE Trans. on Energy Convers.*, vol. 7, no. 3, pp. 418–425, Sep. 1992.
- [5] M.-R. Haghifam and M. Omidvar, "Wind farm modeling in reliability assessment of power system," in *Proc. of PMAPS*, June 2006.
- [6] A. Dobakhshari and M. Fotuhi-Firuzabad, "A reliability model of large wind farms for power system adequacy studies," *IEEE Trans. on Energy Convers.*, vol. 24, no. 3, pp. 792–801, Sep. 2009.
- [7] A. Leite, C. Borges, and D. Falcao, "Probabilistic wind farms generation model for reliability studies applied to Brazilian sites," *IEEE Trans. on Power Syst.*, vol. 21, no. 4, pp. 1493–1501, Nov. 2006.
- [8] A. Ehsani, M. Fotuhi, A. Abbaspour, and A. M. Ranjbar, "An analytical method for the reliability evaluation of wind energy systems," in *Proc. of TENCON*, Nov. 2005.
- [9] X. Liu, S. Islam, A. Chowdhury, and D. Koval, "Reliability evaluation of a wind-diesel-battery hybrid power system," in *Proc. of Industrial and Commercial Power Systems Technical Conf.*, May 2008.
- [10] R. Yokoyama, T. Niimura, and N. Saito, "Modeling and evaluation of supply reliability of microgrids including pv and wind power," in *Proc. IEEE PES General Meeting*, July 2008.
- [11] A. Causebrook, D. Atkinson, and A. Jack, "Fault ride-through of large wind farms using series dynamic braking resistors (March 2007)," *IEEE Trans. on Power Syst.*, vol. 22, no. 3, pp. 966–975, Aug. 2007.
- [12] A. Kasem, E. El-Saadany, H. El-Tamaly, and M. Wahab, "An improved fault ride-through strategy for doubly fed induction generator-based wind turbines," *IET Renewable Power Generation*, vol. 2, no. 4, pp. 201–214, Dec. 2008.
- [13] C. Luo, H. Banakar, B. Shen, and B.-T. Ooi, "Strategies to smooth wind power fluctuations of wind turbine generator," *IEEE Trans. on Energy Convers.*, vol. 22, no. 2, pp. 341–349, June 2007.
- [14] J. Zhao, W. Zhang, Y. He, and J. Hu, "Modeling and control of a wind-turbine-driven DFIG incorporating core saturation during grid voltage dip," in *Proc. of ICEMS*, Oct. 2008.
- [15] Z. Miao, L. Fan, D. Osborn, and S. Yuvarajan, "Control of DFIG based wind generation to improve inter-area oscillation damping," *IEEE Trans. on Energy Convers.*, vol. 24, pp. 415–442, June 2009.
- [16] P. Tavner, G. van Bussel, and F. Spinato, "Machine and converter reliabilities in wind turbines," in *Proc. of International Conference on Power Electronics, Machines and Drives*, Apr. 2006.
- [17] M. Arifujjaman, M. Iqbal, and J. Quaicoe, "A comparative study of the reliability of the power electronics in grid connected small wind turbine systems," in *Proc. of Canadian Conference on Electrical and Computer Engineering*, May 2009.
- [18] G. Joos, B. Ooi, D. McGillis, F. Galiana, and R. Marceau, "The potential of distributed generation to provide ancillary services," in *Proc. of Power Engineering Society Summer Meeting. IEEE*, vol. 3, Seattle, WA, 2000.
- [19] T. Ackermann, *Wind Power in Power Systems*. Chichester, UK: John Wiley and Sons, 2005.
- [20] V. Akhmatov, *Induction Generators for Wind Power*. Brentwood, UK: Multi-Science Publishing Company, 2005.
- [21] G. Grimmett and D. Stirzaker, *Probability and Random Processes*, 3rd ed. Oxford, UK: Oxford University Press, 2001.
- [22] A. Domínguez-García, J. Kassakian, and J. Schindall, "A generalized fault coverage model for linear time-invariant systems," *IEEE Trans. on Reliab.*, vol. 58, no. 3, pp. 553–567, September 2009.
- [23] J. Endrenyi, *Reliability Modeling in Electric Power Systems*. Hoboken, NJ: Wiley-Interscience, 1978.
- [24] G. Masters, *Renewable and Efficient Electric Power Systems*. Hoboken, NH: Wiley-Interscience, 2004.
- [25] S. Asmussen and P. W. Glynn, *Stochastic Simulation: Algorithms and Analysis*. New York, NY: Springer, 2007.
- [26] "An Assessment of Distribution System Power Quality," EPRI, Palo Alto, CA, Tech. Rep. TR 106294, May 1996.
- [27] A. Bazzi, A. A. Domínguez-García, and P. Krein, "A method for impact assessment of faults on the performance of field-oriented control drives: A first step to reliability modeling," in *Proc. of IEEE APEC*, Palm Springs, CA, 2010.